NASA

Report Documentation Page

1. Report No.	2. Government Accession No.	3. Recipient's Catalog No.

4. Title and Subtitle
Phase Diversity and Space Based Imaging

5. Report Date

6. Performing Organization Code

7. Author(s)
Richard G. Lyon

8. Performing Organization Report No.

10. Work Unit No.

9. Performing Organization Name and Address
University of Maryland Baltimore County
302 Administrative Building, 1000 Hilltop Circle
Baltimore, Maryland 21250-5394

11. Contract or Grant No. NAS5-32337
USRA subcontract No. 5555-44

12. Sponsoring Agency Name and Address
National Aeronautics and Space Administration
Washington, DC 20546-0001
NASA Goddard Space Flight Center
Greenbelt, MD 20771

13. Type of Report and Period Covered Final
June 1995 - July 2000

14. Sponsoring Agency Code

15. Supplementary Notes
This work was performed under a subcontract issued by
Universities Space Research Association
10227 Wincopin Circle, Suite 212
Columbia, MD 21044 Task 57

16. Abstract

The efforts of this report concentrate on the design, development and application of massively parallel model based, image processing algorithms to deconvolve, reconstruct, or enhance degraded imagery. Algorithms have been developed to deconvolve the optical response function from a noisy or corrupted image or set of images. The algorithms have been applied to Hubble Space Telescope (HST) Faint Object Camera (FOC) imagery, to the Solar and Heliospheric Observatory (SOHO) Large Angle Spectrometric Coronagraph (LASCO) imagery as well as groung based hyperspectral Fabry-Perot etalon 3D data cubes.

17. Key Words (Suggested by Author(s))	18. Distribution Statement
Image processing	Unclassified--Unlimited

19. Security Classif. (of this report)	20. Security Classif. (of this page)	21. No. of Pages	22. Price
Unclassified	Unclassified	1	

NASA Form 1626 Oct 86

Serial report 57

Phase Diversity and Space Based Imaging

R.G. Lyon

NASA - Goddard Space Flight Center

Abstract

Space based imaging systems require increasingly large apertures to keep pace with the demand for higher spatial resolution imagery for Earth and Space sciences missions. This is so because optical telescope resolution (i.e., the smallest detail to be discerned) is proportional to the ratio of the observed wavelength and the diameter of the aperture. Note that the higher the resolution the smaller the ratio of observed wavelength and telescope diameter. Weight and cost becomes increasingly prohibitive for deploying single telescope mirrors in space with apertures greater than a few meters. Hence, rather than sending one large monolithic aperture aloft, one solution is to send several smaller apertures that can be deployed in a suitable configuration in orbit. One such configuration is simply a segmented filled-aperture system comprised of several small apertures that fit closely together to simulate one large aperture; obviously these apertures must be accurately aligned to work in concert. Alternatively, another similar configuration could be a non-filled-aperture (i.e. sparse-aperture systems) that have several apertures with gaps between each aperture element; such a configuration can have the same resolution as the former one as long as the maximum diameters of the two configuration are the same; the gaps in this configuration simply represent areas where no flux is collected. Another level of sophistication would be to launch an interferometric imaging system comprised of two or more small apertures; however, this system requires a level of communication between aperture elements that can be daunting in terms of achieving a final image. The commonality of these techniques lies in increased reliance on sophisticated computational and information theoretic techniques in order to align, maintain alignment and recover a high quality image. This can be accomplished by technique known as phase diversity. We discuss each of these imaging systems, show examples and develop phase diversity for each system.

1. INTRODUCTION

NASA's Origins [1] and New Millennium [2] programs require large space based imaging systems. These imaging systems will be interferometric imaging systems (Submillimeter Probe of Evolutionary Cosmic Background - SPECS), segmented aperture telescopes (Next Generation Space Telescope - NGST) or sparse aperture systems (Terrestrial Planet Finder - TPF) . Most of these systems will require wavefront sensing (WFS) and optical control systems (OCS) because of weight, deployment, thermal, structural, and dynamics, and some may require substantial post-processing to obtain the desired image quality. Each of these imaging systems requires complex algorithms and computer processing. For example an imaging interferometer must convert from the observed visibility functions to the "dirty" image and the dirty image must undergo subsequent deconvolution/enhancement to obtain the "cleaned" image. Segmented aperture systems require WFS methods such as phase retrieval and/or phase diversity and an active optical control system for initial alignment and to maintain alignment over the mission life. Finally sparse aperture systems may also require WFS methods and an active optical system with enhancement/deconvolution to clean the resultant image.

Most of NASA's previous space-based imaging systems have relied on a "monolithic" telescope design examples of which are the Hubble Space Telescope (HST) and the to be launched Space Infrared Telescope Facility (SIRTF). Monolithic, as defined here, means a telescope with a single piece primary mirror. This has the advantage that the mirror is generally ground, polished, integrated, aligned, tested and deployed as a single piece of material, and in flight, the mirror is generally thermally and structurally stable. The mirror size is determined, ideally, by the desired science return, however, it is also severely constrained by cost, weight, size and ability to manufacture, test and must be able to fit into available launch vehicles. However, it has become increasingly obvious that we must quantitatively evaluate the aforementioned new technology telescope configurations for high resolution images. Herein we develop a generalized imaging model and develop each of these telescope configurations within the model. Shown will

be a simulation of each as well as wavefront sensing, optical control and deconvolution methods. We also develop phase diversity to both determine the source of errors, i.e. estimate the wavefront and to boost the spatial frequency response of the telescope.

2. GENERALIZED IMAGING MODEL

An observed noisy image, d(x,y), can be represented by:

$$d(x,y) = PSF(x,y;A,\phi) ** O(x,y) + \eta(x,y) \tag{1}$$

where PSF(x,y) is the optical point spread function, which is how the telescope performs with regards to a point source of light. O(x,y) is the object, $\eta(x,y)$ is the noise associated with the object signal and telescope system including detectors and (x,y) represent the image plane coordinates. The PSF can be calculated as the two dimensional Fourier transform of the complex pupil function [3].

$$PSF(x,y,A,\phi) = \left| \frac{1}{\lambda F} \iint A(u,v)\ \exp[i\phi(u,v)]\ \exp\left[-i2\pi \left(\frac{xu}{\lambda F} + \frac{yv}{\lambda F} \right) \right] dudv \right|^2 \tag{2}$$

A(u,v) represents the aperture mask of the pupil function, (u,v) are the spatial coordinates in the system exit pupil. A(u,v) is the amplitude within the aperture and zero outside. $\phi(u,v)$ is the phase delay at each point in the system exit pupil. λ and F represent the wavelength and system focal length respectively.

We see that the PSF is the modulus squared of the 2D Fourier transform of the complex pupil function defined as $P(u,v) = A(u,v)e^{i\phi(u,v)}$. If we define $u = \lambda F f_x$ and $v = \lambda F f_y$ then the optical transfer function (OTF) is given by the Fourier transform of equation (2):

$$OTF(f_x,f_y) = \frac{P(f_x,f_y) \otimes P(f_x,f_y)}{P(f_x,f_y) \otimes P(f_x,f_y)\big|_{f_x=f_y=0}}$$

(3)

and the observed monochromatic image in the Fourier domain by:

$$\tilde{d}(f_x, f_y) = OTF(f_x, f_y)\tilde{O}(f_x, f_y) + \tilde{\eta}(f_x, f_y) \quad (4)$$

The imaging operation is a low pass filter [put in plot here]. For a given aperture it can be shown that the highest frequency response filter is given when the phase, $\phi(u,v)$, is equal to zero. In a well designed optical system the rms. of the phase is less than $\lambda/20$ (i.e. the wavefront in the aperture is configured to this specifically) and represents a "diffraction limited" system. Even with zero phase the OTF is "compactly supported" i.e., the autocorrelation in equation (3) is non-zero over only a finite region. Thus any optical system is, at best, a low-pass spatial filter which passes only a limited amount of information to the focal plane. Image restoration methods a.k.a. deconvolution, are an attempt to boost the response of the spatial filter below the cutoff frequency implicitly defined by equation (3). Super-resolution is an attempt to analytically continue the spatial frequency content beyond the optical cutoff frequency, a much harder proposition and attained in only in a limited number of cases to date.

The above imaging model, represented by equations (1) through (4) is the same for a monolithic, segmented, sparse or an interferometric imaging system. What changes, in each of these cases, is the aperture and phase functions and hence the point spread function and optical transfer function. For a given aperture size the OTF has the same optical cutoff frequency for the monolithic, segmented, sparse and interferometric systems. However, the details of how the filter rolls off to the cutoff frequency is different in each case and can result in very different image quality.

Residual design errors, misalignments, deformations and temporal dynamics caused by thermal and structural effects cause the phase function, $\phi(u,v)$, to be non-zero, and possibly time dependent resulting in lower fidelity imaging. If the phase function can be determined then it may be possible to correct these sources of errors. Wavefront sensing

is the method by which one determines the phase and an optical control system is what uses the phase function to correct the system by moving and/or deforming the optics and ideally driving the phase function to zero.

In the following sections we show the PSFs , OTFs and a simulated image for the monolithic, segmented, sparse and interferometric imaging cases and discuss their differences as well as discuss wavefront sensing and optical control and deconvolution.

The telescopes angular resolution scales as λ/D, where D is the diameter of the primary mirror and λ is the wavelength. High resolution implies a large diameter mirror, however, does not necessarily imply that we use a filled aperture. The segmented, sparse and interferometric imaging systems are methods to overcome using a single large optic, however, wavefront sensing, optical control and/or post-processing may be required.

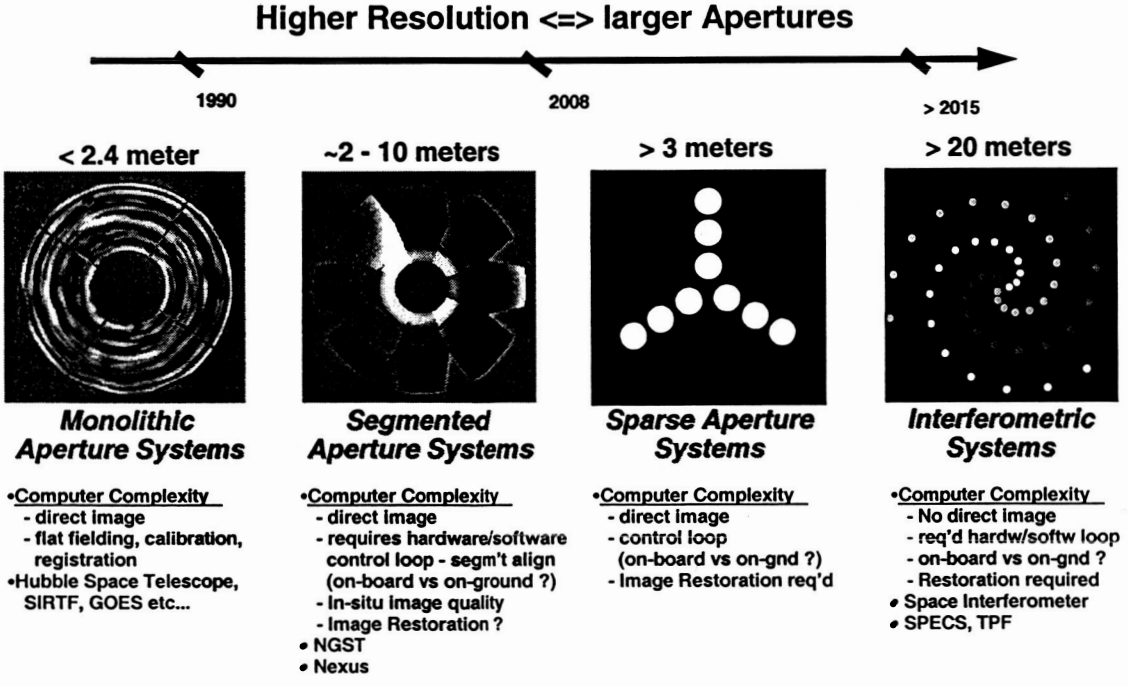

3. MONOLITHIC, SEGMENTED, AND SPARSE APERTURE IMAGING

Monolithic Imaging Systems

The leftmost image of Figure 1 shows the Hubble Space Telescope primary mirror [3] as an example of a monolithic mirror. The residual polish marks are shown as light and dark regions, where white is too high and black too low. For space applications, it is possible to reach apertures of 2-3 meters with this type of configuration, however the cost and weight is high. Little post-processing must be performed on the resulting image for useable science. Typical processing would include flat-fielding, (i.e. correcting for detector errors over the image plane), calibration, (i.e. conversion to radiometric units) and possibly image registration.

Segmented Imaging Systems

The second picture from the left in Figure 1 shows a simulation of an 8 meter segmented deployable telescope primary mirror [4], one possible design for the Next Generation Space Telescope (NGST). Segmented since each of the 9 petals (1 center and 8 edge segments) are actually manufactured as separate mirrors. Deployable implies that the segments fold up to fit in the launch vehicle and are unfurled (deployed) after launch, and locked into position. This configuration has the advantage that a larger telescope can be built to fit into a smaller payload. However the segments much be first deployed, then aligned and the alignment must be maintained throughout the mission life. Furthermore the configuration is generally less structurally and thermally stable than the monolith. This generally requires an active optical control system [4][5], requiring much more computational complexity.

Sparse Aperture Imaging Systems

The third picture from the left in Figure 1 is a sparse aperture configuration. It may be realized a number of different ways in hardware. Each of the white circles can represent a piece of the same mirror, or separate telescopes mounted on the same structure, or, they could be entirely separate telescopes which are tethered together or as "free flyers", i.e. a constellation of telescopes. If the apertures are not part of the same rigid, thermally stable structure, then an active control loop may be required to maintain alignment of the

sub-apertures[6][7]. In a sparse aperture configuration, the aperture locations are fixed both in number and position. Sparse aperture configurations typically give a lower quality image than both the monolithic and segmented configuration, however the overall aperture can be much larger in principle. The image quality usually increases with increasing number of sub-apertures. Note that the total area of the sub-apertures is smaller than a full aperture case, thereby sacrificing the light gathering ability, i.e. the sensitivity. The typical low image quality of these sparse aperture imaging systems generally requires post-processing such as image restoration and/or enhancement [10] and may also require some wavefront sensing and optical control to maintain alignment of the sub-apertures.

Interferometric Imaging Systems

The rightmost picture in Figure 1 shows a simulated interferometric imaging system. Each of the 3 different gray scales corresponds to a separate telescope system. In this simulation there are 3 separate telescope systems which are moved in time. At each temporal position a separate image is collected in it's Fourier domain. These sub-images are mosaiced together in the Fourier domain and inverse Fourier transformed to obtain the synthesized image. These type of systems can, in principle, be very large, (e.g., 100's of meter,) (VLA ???) since each of the telescopes could be separately launched and subsequently aligned, i.e. "phased" together in space [8][9]. This type system may also require active metrology hardware and/or an active control loop. This active metrology hardware would determine the relative aperture locations, since this knowledge is required to create an image. Furthermore an active optical system may be required to maintain alignment of each individual telescope during the collection time. Although the image resolution can be extremely high, the image quality can still be relatively poor. It also generally has a very small field of view. Post processing of the resultant image is always required.

The top row of Figure 2 shows, on a logarithmic scale, a monolithic, a segmented and a sparse aperture observed PSFs. Each system is an aperture of 1 meter. The monolithic

PSF is circularly symmetric. The segmented PSF shows large diffraction flares, diffracting energy out of the core. The sparse PSF is relatively large with much less relative energy in the core. The bottom row shows their respective optical transfer functions on a linear scale. The monolithic PSF falls off from the core and shows much more modulation away from the center. The segmented falls off faster than the monolithic case and has a cutoff frequency which is a weak function of direction. The sparse OTF falls of quickly and is strongly dependent on direction. Note that all the OTFs have approximately the same area over which they are non-zero.

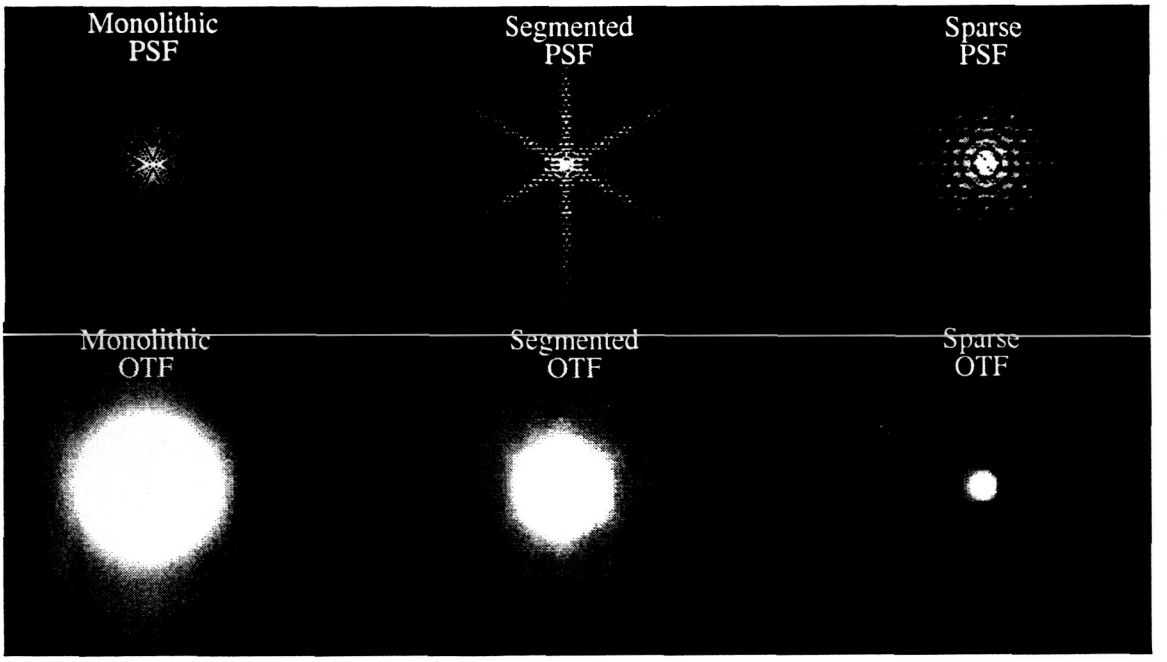

Figure 2
Simulated PSFs and OTFs for Each Configuration

Figure 3 shows a simulated image of Saturn with a monolithic, segmented and sparse aperture system. The monolithic image appears the sharpest, the segmented is slightly less sharp and the sparse is noticeably more blurry. Figure 4 shows slices through the power spectral densities, on a log-linear scale, for the true image and the monolithic, segmented and sparse imaging cases. The cutoff frequency is easily seen where the power drops sharply and is nearly the same for all the imaging cases except the true image, i.e., how the object would be seen if the telescope were perfect. However, below the cutoff frequency, the modulation varies by 2 orders of magnitude with the lowest for the sparse case and the best for the monolithic.

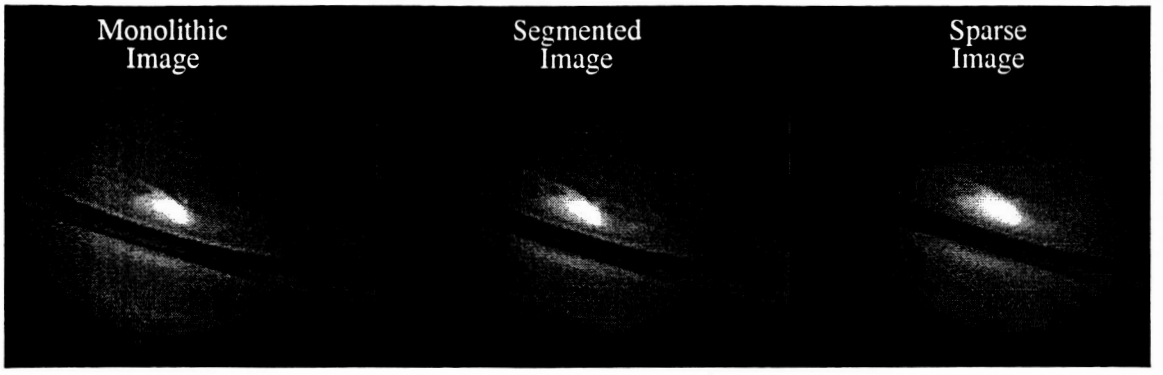

Figure 3
Simulated Images for Each Configuration

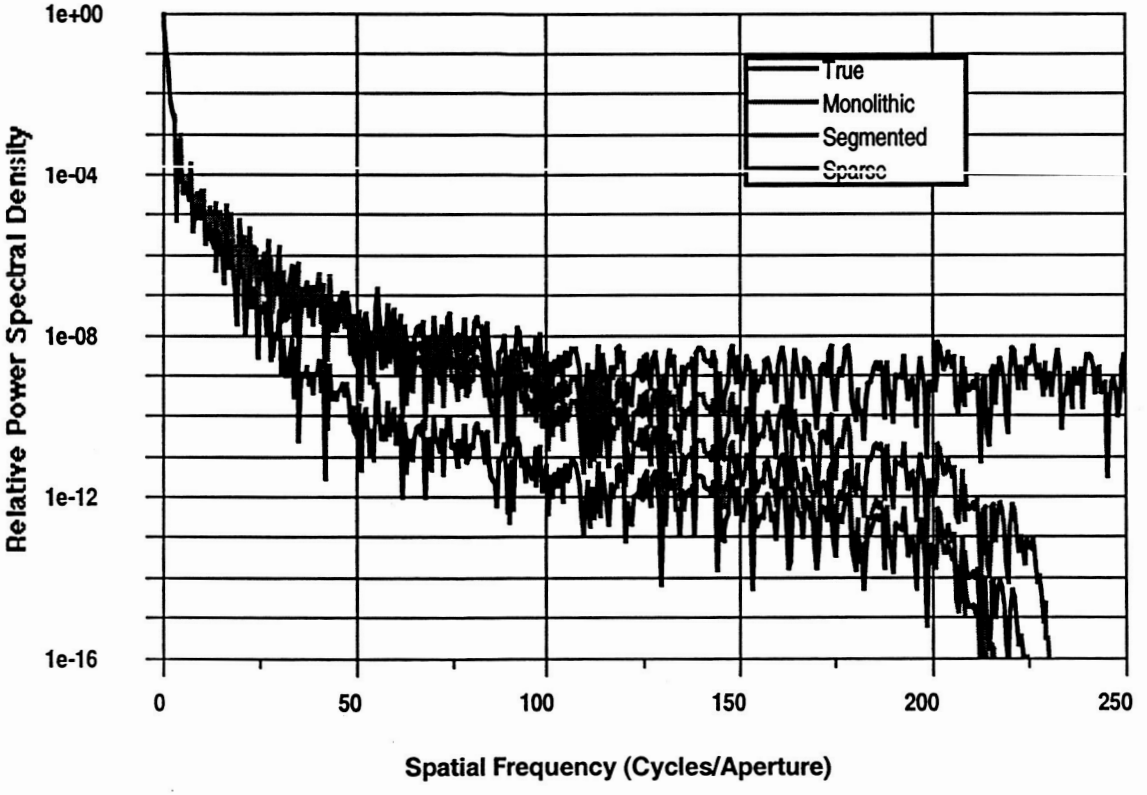

Figure 4
Saturn Image Power Spectral Densities

4. PHASE DIVERSITY

Model-based image processing methods can be used to deconvolve, or reconstruct imagery, and phase retrieval methods can be used to determine the wavefront error in an optical system. At first glance these might seem mutually exclusive, however, such methods are tightly coupled. Image deconvolution requires the optical response of the system, i.e., the point spread function (PSF), and generally this is not accurately known due to incomplete knowledge of the on-orbit errors and misalignments. Thus, one desires to determine the object signature without completely knowing the system that created it. Determination of the errors (phase retrieval) and the deconvolution (object estimation) problems can be cast into a symbiotic hardware/software relationship requiring the use of only one methodology, known as Phase Diversity. Thus, one can recast the imaging problem as a tightly coupled phase retrieval and image deconvolution problem inherently tied to the optical system either via phase retrieval or the use of active optics. It is this *Phase Diversity* which will be discussed with regards to the aforementioned optical system configurations.

Phase diversity is a method which uses multiple observed imagery, (e.g., the Earth or extended astronomical objects), with a high fidelity model to obtain an optical system. These input images are coupled to an inverse wave propagation algorithm, based on nonlinear optimization theory, to determine the phase function and hence the mirror shapes and misalignments, as well as estimate the object, i.e. boost the spatial frequency response. Phase diversity will work with all the aforementioned mirror configurations and is still a current area of research. Phase diversity is directly useful to determine the on-orbit design as well as thermal/structural deformations, misalignments and potential rapidly varying dynamic errors of space based imaging systems. Determination of these would allow for an active optical control system to correct the errors on-orbit, thereby, allowing for larger and lower cost mirrors than current monolithic mirror technology.

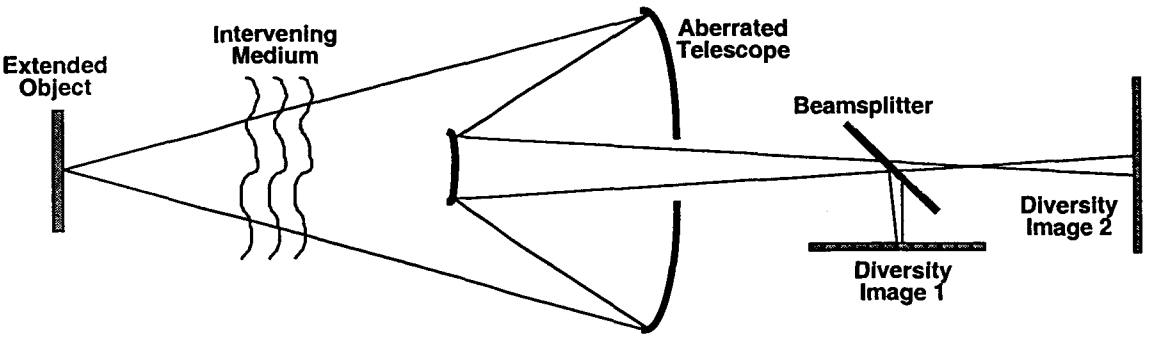

Figure 5
Conceptual Phase Diversity Imaging System

Figure 5 shows a conceptual optical schematic of a phase diversity system; both the telescope and the intervening medium contribute to the phase function of the entire system. The telescope contributes by deterministic design residuals, and the unknown, but fixed, misalignments, fabrication errors, surface scatter and thermal/mechanical drift; the atmosphere contributes by thermally induced, mullet-layer, density changes contributing to stochastic phase fluctuations. In figure 5 the phase diversity is introduced via a device to split the beam into two, or more, separate channels, each of which sees a large, known, phase aberration such as focus. The telescope and atmospheric aberrations occur in both channels, common mode, while only the diversity is dissimilar each channel. Note that although focus is used in this simplified schematic it is not the only choice. The optimal choice of phase function introduced is as yet unknown. The phase diversity method solution uniqueness, convergence properties and accuracy are still under study. The phase diversity problem is a rich research problem with potential applications in future NASA missions. Towards this end, OSCAR has been researching, developing and enhancing different methods and attempting to quantify their accuracy, precision and range for each of the aperture configurations. Furthermore we are developing an experimental prototype benchtop system to research the problem in a controlled fashion. The goal being introduce and to a multitude of real world effects, at first, in an open loop fashion and to ultimately develop a closed loop optical control system. The primary limitations for closed loop control are a trade between accuracy/precision and

computational requirements. We have also been applying massively parallel and fault tolerant processing techniques to these methods.

Figure 6 shows a simulation of phase diversity for a monolithic aperture system. We introduced focus diversity into a 2 channel imaging system. The top image shows the "true" extended object followed by images through channels 1 and 2 of a phase diverse imaging system. These 2 images are input, along with an optical systems model, to a phase diversity algorithm. This algorithm estimates both the phase function and the object. If we use and active optical control loop we can minimize this phase function giving an even higher quality image.

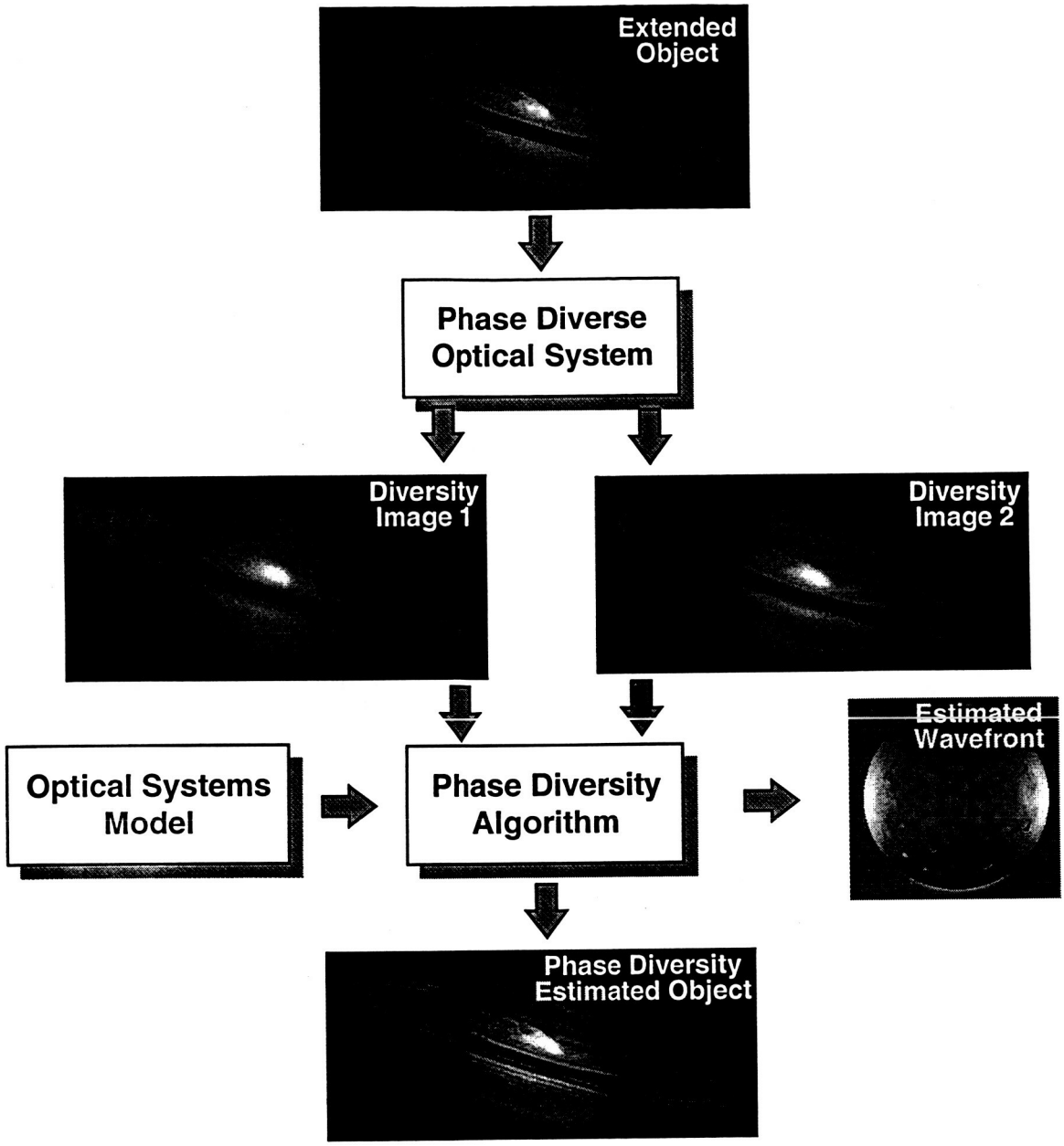

Figure 6
Phase Diverse Imaging Simulation

5. SUMMARY AND FUTURE WORK

In summary, we have given an overview of the different types of imaging systems applicable to future NASA space imaging systems for both Earth and Space sciences missions. We have developed a comprehensive modeling package to model these systems

and have the capability to include, diffraction, phase aberrations, scattering, sampling, finite detector size, photon and gaussian noise as well as model wavefront sensing including phase retrieval and phase diversity and optical control techniques for both open and closed loop. We have shown simulations for the monolithic, segmented, and sparse apertures imaging systems and a phase diversity simulation. We are preparing the quantitative results for publication.

6. REFERENCES

(1) See http://origins.jpl.nasa.gov

(2) See http://nmp.jpl.nasa.gov/index_menu.html

(3) Lyon, R. G., Dorband, J. E., Hollis, J. M., "Hubble Space Telescope Faint Object Camera Calculated Point Spread Functions", *Applied Optics*, *36*, No. 8 (1997).

(4) Lyon, R. G., Hollis, J. M, Dorband, J., Murphy, T.P., "Extrapolating HST Lessons to NGST", *Optics and Photonics News*, Vol. 9, No. 7 (1998)

(5) Redding, D., Basinger, S., Bely, P., Burg, R. Lyon, R. G., Mosier, G., Femiano, M., "Phasing of a Segmented Aperture Telescope in Space", Proceedings of SPIE (Poster Paper), Vol. 3356, Kona Hawaii, March 1998

(6) DeYoung,D.B., Dillow,J., Corcoran,S., Andrews,E.V., Yellowhair, J., Devries, K..,"Ground Demonstration of an Optical Control System for a Space-Based Sparse Aperture Telescope", Proc. SPIE Vol. 3381, p. 181-192, Airborne Laser Advanced Technology, 09/1998

(7) DeYoung, D.B., Deshetler, D.B.,Kvasnack, M.A., "Low-cost space structure experiment optical phasing control system", Proc. SPIE Vol. 2478, p. 117-127, 06/1995

(8) Leisawitz, D.; Mather, J. C.; Moseley, S. H. _Jr.; Danchi, W.; Dwek, E.; Gezari, D.; Pedelty, J. Silverberg, R.; Staguhn, J.; Yorke, H.; Zhang, X.,"The Uniqueness Space for SPIRIT and SPECS", American Astronomical Society Meeting 195, #88.07, 12/1999

(9) Leisawitz, David; Mather, John C.; Moseley, S. Harvey, Jr.; Dwek, Eli; Feinberg, Lee; Hacking, Perry; Harwit, Martin; Mundy, Lee G.; Mushotzky, Richard F.; Neufeld, David; Spergel, David; Wright, Edward L., "The Submillimeter Probe of the Evolution of Cosmic Structure (SPECS)", The Physics and Chemistry of the

Interstellar Medium, Proceedings of the 3rd Cologne-Zermatt Symposium, held in Zermatt, September 22-25, 1998

(10) Lyon, R. G., Hollis, J. M, Dorband, J. E., "A Maximum Entropy Method with A Priori Maximum Likelihood Constraints", *Ap.J., 478,* 658-662 (1997).

Timothy Murphy

University of Maryland Baltimore County
Department of Computer Science and Electrical Engineering
murphy@albert.gsfc.nasa.gov

Task 57

Mr. Murphy's portion of this task involves designing an active, fault tolerant, on-board, optical control system (OCS) for the Next Generation Space Telescope (NGST). The OCS will use phase retrieval methods that require substantial on-board compute power. The OCS will be used to perform the initial optical alignments as well as periodic optical alignments. Mr. Murphy has also been charged with conceptualizing, designing, developing, coding, testing, benchmarking, document, and delivering prototypical algorithms/software for the control system.

Optical Alignment and Control for NGST: Prototype Application for Fault Tolerant Computing in Space

As part of NASA's Remote Exploration and Experimentation (REE) program we have supplied prototype scalable, multiprocessor computer applications for optical alignment and control of the Next Generation Space Telescope (NGST) [1]. These applications are to be run on the REE fault tolerant computing testbed. The 1999 CESDIS Annual Report (NASA NP-1999-11-186-GSFC) describes the motivations for research into fault tolerant computing in space with commercial microprocessor.

A Misell phase retrieval algorithm, used to determine the telescope wavefront from a set of unresolved images of point sources, was originally delivered to the REE project in FY'98. A first revision of the Misell code was delivered in December 1998, with updates in January and September 1999, and March and June 2000. This algorithm produces the wavefront as the argument of a complex valued image, thus its values are restricted to (wrapped) the range $-\pi$ to $+\pi$. In December of 1998 we delivered a single processor phase unwrapping algorithm, which restores the full range of values to the wavefront by identifying and removing 2π discontinuities. The actuator fitting program, act_fit, takes an unwrapped wavefront and a file containing telescope parameters as input, and creates a file of actuator positions to minimize the least-squared wavefront error.

Our group has developed, tested and delivered actuator fitting code, which determines the optimal actuator motions from a wavefront, for the primary and deformable mirrors. This code was developed on the 128 processor Hive computer at Goddard Space Flight Center and delivered in February of 1999, with an update in June 2000.

We have provided for actuators on deformable mirrors (DM) and actuators which move primary mirror (PM) segments in piston, tip and tilt. It is assumed that each actuator has a linear response, referred to as its influence function, on the wavefront. The influence functions are calculated from a set of parameters. Specifically, the DM actuators have a coefficient that describes their region of influence and a file containing the mapping of actuator centers onto the telescope's exit pupil. The PM actuators govern piston, tip and tilt for each PM segment.

Figure 1 shows a 512 x 512 wavefront before and after correction by a 349 actuator DM and PM segments. Figure 2 shows a 1024 x 1024 wavefront before and after correction with a 3152 actuator DM. The 3152 actuator map was created by placing actuators on a 64 x 64 grid and eliminating those with centers substantially off the pupil. The images in figure 2 are contrast enhanced to better show the wavefront features.

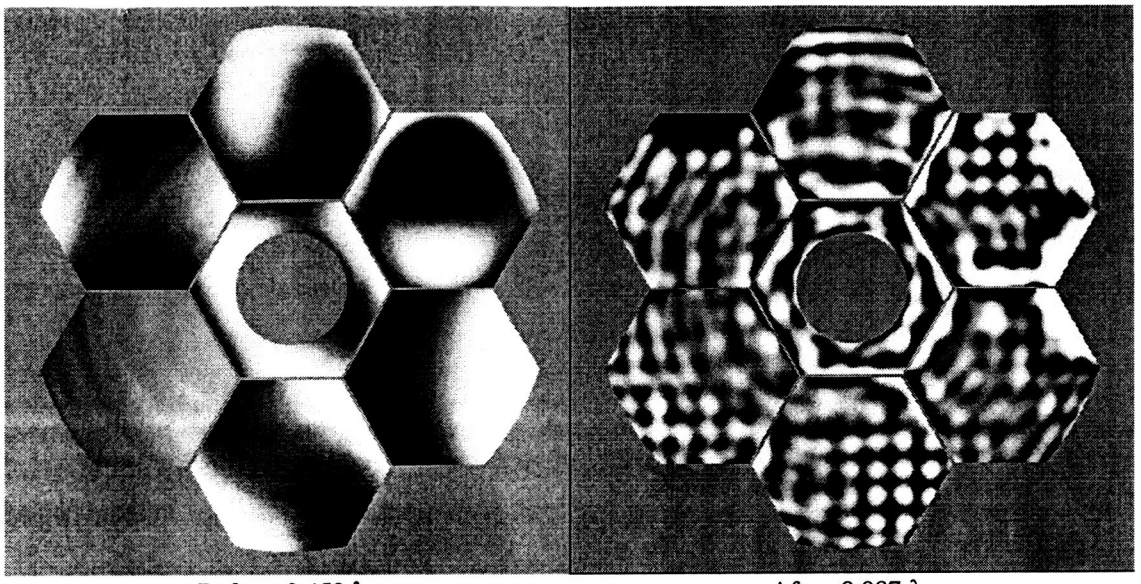

Before: 0.453 λ rms After: 0.087 λ rms

Figure 1. Sample wavefront corrected by 349 DM actuators and PM segments

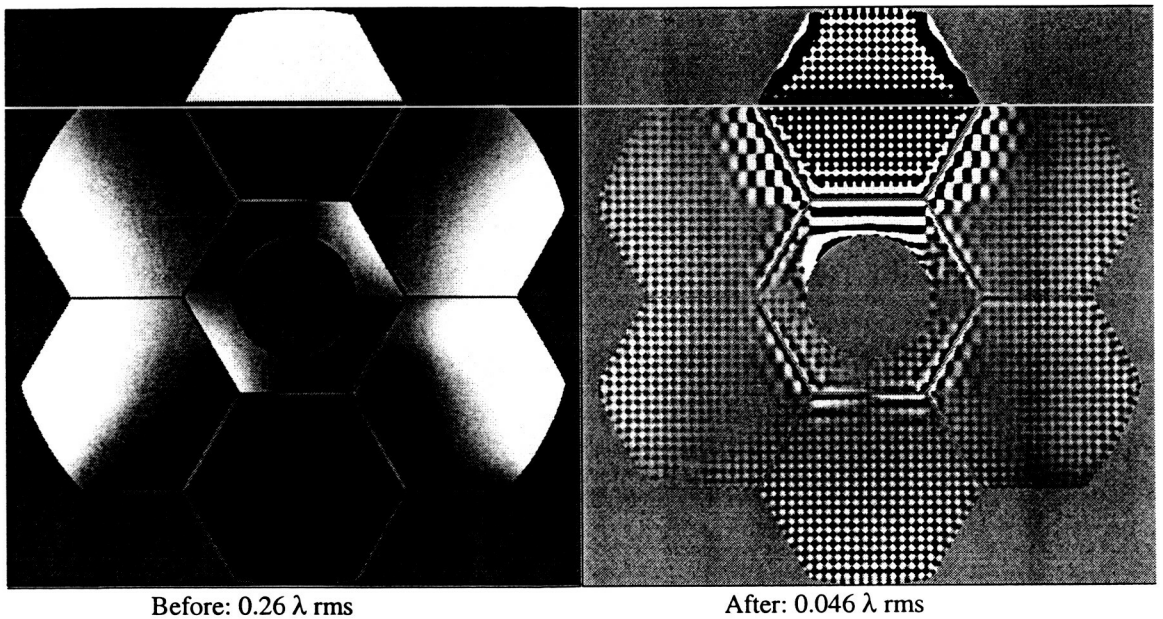

Before: 0.26 λ rms After: 0.046 λ rms

Figure 2. Sample wavefront corrected by 3152 actuator DM.

The NGST optical control software will most likely require calibration and explicit storage of the influence function matrix rather than the parametric description of the matrix used in act_fit. This storage will be 349 MB just for a 349 actuator DM. If a PM with deformable segments is used, the required storage is several gigabytes. Such a large storage requirement adds to the mission cost and power and decreases the speed of calculation. We developed code to exploit sparse actuator fitting matrices. The algorithm to generate the sparse matrix retains those matrix elements greatest in magnitude while keeping the minimizing the change in the sum of the elements of each row [2]. Figure 3 shows the relative rms wavefront error after correction for the sparse matrices as a function of ρ, the fraction of the original matrix elements retained in the sparse matrix. Very little increase in error occurs until ρ is smaller than 0.2. Research continues to find optimal ways of selecting matrix elements to discard in forming the sparse matrix.

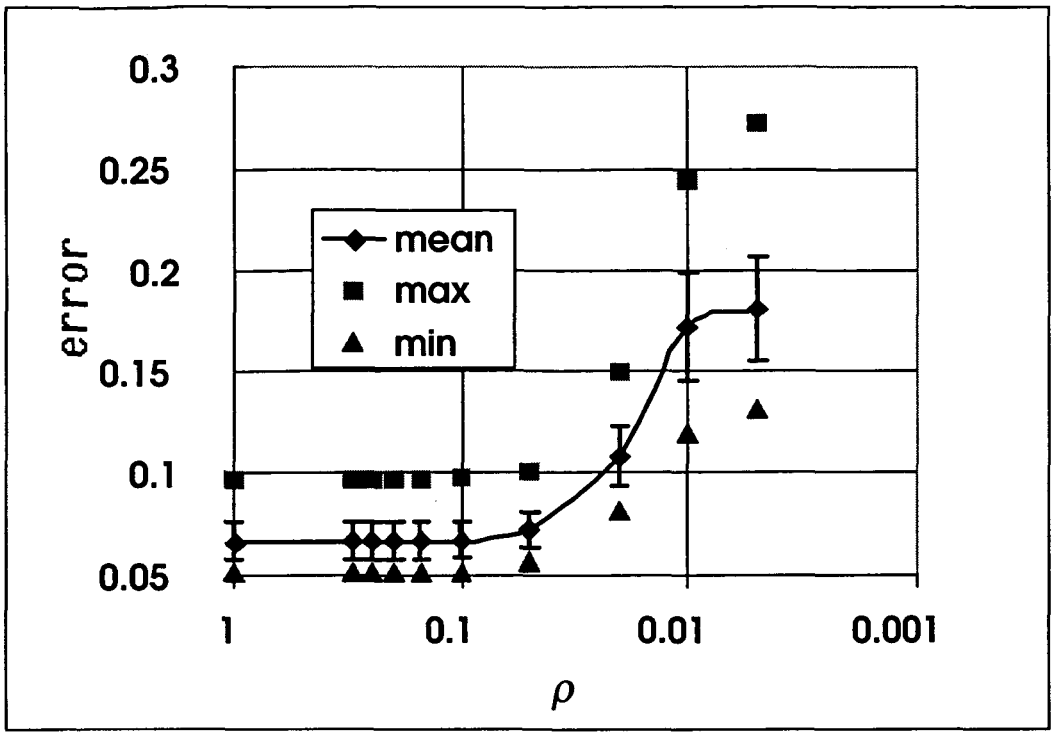

Figure 3.

References

(11)Stockman, H. S. Ed. (1997). *The Next Generation Space Telescope.* Association of Universities for Research in Astronomy, Inc.

(12)Murphy, T. P., Lyon, R.G., Dorband, J.E., and J. M. Hollis, "Sparse Matrix Approximation Method for Phase Retrieval Based Active Optical Control System," Workshop on Computational Optics and Imaging for Space Applications, Greenbelt, MD, May 2000.